

Onset and Suppression of Collective Oscillations: Interplay of Diversity, Noise and Coupling Delay

Vladimir Klinshov*

*Institute of Applied Physics of the Russian Academy of Sciences,
46 Ulyanov Street, 603950 Nizhny Novgorod, Russia*

Igor Franović†

*Scientific Computing Laboratory, Center for the Study of Complex Systems,
Institute of Physics Belgrade, University of Belgrade, Pregrevica 118, 11080 Belgrade, Serbia*

(Dated: July 6, 2022)

We consider the onset and the suppression of macroscopic oscillations in a heterogeneous assembly of active rotators influenced by noise and coupling delay. The key model ingredients, including the interplay of diversity (manifested as excitable or oscillatory local dynamics), noise and delay are typically found in neuronal and other biophysical systems. We study the noise- and delay-free setup within the framework of Ott-Antonsen reduction method, analytically determining the state with a constant mean field and its stability boundaries in terms of the mean and the variance of the frequency distribution. We establish that the system may exhibit three macroscopic regimes, namely the rest state, the synchronous state and the asynchronous state, whereby the transitions between them are organized via a SNIPER and a Hopf bifurcation of the collective dynamics. It is numerically demonstrated that this basic bifurcation structure remains qualitatively the same in presence of noise and coupling delay. Nevertheless, the noise is found to shift both of the relevant bifurcations to smaller diversity: on one hand, it promotes the onset of the collective mode, effectively reducing the critical diversity associated to the SNIPER bifurcation, but on the other hand, it also introduces disorder, which enforces the transition from synchronous to asynchronous regime in less heterogeneous assemblies. The coupling delay is established to have a stabilizing effect on the rest state, effectively quenching the collective mode by decreasing the critical diversity related to the Hopf bifurcation.

I. INTRODUCTION

The onset of a collective mode mediated via a transition to synchrony is a fundamental paradigm of macroscopic behavior in a broad variety of fields, ranging from neuroscience and other biologically-inspired models to chemistry, technology and social science [1, 2]. A classical approach within the theory of nonlinear dynamics is to regard populations exhibiting a collective mode as macroscopic oscillators [3–5], which can then interact with other populations or be subjected to external stimuli. In the present study, we investigate how the emergence of synchrony is influenced by the interplay of diversity, coupling delay and noise, the three ingredients characteristic for neuronal and other biophysical systems [6, 7]. The simultaneous presence of these three factors in models of real-world systems comes in a natural way [8]. For example, in many cases the active elements are not self-oscillating, but rather excitable units, whereby due to variability [9–12], it is further more realistic to consider heterogeneous instead of homogeneous assemblies. Depending on the particular context, variability may alternatively be referred to as diversity, heterogeneity, impurities, or quenched noise. Moreover, one often has to introduce explicit coupling delay in order to de-

scribe the effect of finite velocity of signal propagation or the latency in information processing [7, 13–17], whereas creating coarse-grained models inevitably requires one to incorporate different sources of noise [18–25]. While the independent or combined effects of several of these ingredients have been extensively explored, their co-effects are yet to be understood.

In particular, within the classical Kuramoto paradigm, it is shown that the continuous (second-order) transition to synchrony occurs once the coupling between the phase oscillators becomes strong enough to overcome the effects of diversity [2, 26]. Nevertheless, diversity alone has been shown to be capable, under appropriate conditions, to enhance the response of an assembly to external forcing or to promote synchronization [10, 11, 27]. Moreover, in case of heterogeneous assemblies comprised of excitable and oscillatory units rather than the phase oscillators, it has been demonstrated that the transition to synchrony with increasing diversity may be classical or reentrant, depending on the particular form of the frequency distribution of single units [28]. For such a setup, it has also been indicated that the collective firing emerges via a generic mechanism where the entrainment of units is degraded either via increasing diversity or noise [11]. In systems consisting just of excitable units, it is well known that the noise may play a constructive role, contributing to the onset of collective firing via synchronization of local noise-induced oscillations [29–32]. Regarding the effect of coupling delay, it has been

* vladimir.klinshov@ipfran.ru

† franovic@ipb.ac.rs

demonstrated in the case of standard Kuramoto model with uniform delays that the transition between the incoherent and coherent states is in general discontinuous instead of continuous, and that the synchronization frequency is suppressed by the delay [26, 33]. The qualitative analysis of the collective dynamics of assemblies of sine-coupled oscillators without coupling delay primarily relies on the Ott-Antonsen reduction method [34, 35], based on the Ansatz that the long-term macroscopic dynamics of such systems settles on a particular invariant attractive manifold. Only quite recently, an approach involving the so-called circular cumulants [36, 37] has been developed to incorporate a first-order correction to the Ott-Antonsen theory which accommodates for the effects of noise. Nonetheless, an effective theory that can account for the combined effects of noise and diversity within the Ott-Antonsen framework is still lacking.

Given the stated above, our approach to analysis of the combined effects of diversity, coupling delay and noise consists in the following. We first provide an exact description of a heterogeneous population of excitable and oscillatory units in the delay- and noise-free setup within the Ott-Antonsen framework, determining the macroscopic stationary state, characterized by a *constant mean-field*, and the bifurcations outlining its stability boundaries. The stationary state and the associated self-consistency equation are determined for an arbitrary distribution of natural frequencies, but the subsequent bifurcation analysis refers to the case of a uniform frequency distribution on a bounded interval, which has the advantage of allowing for a complete analytical treatment. Having established the basic bifurcation scenario for the onset and the suppression of the collective mode, which involves a SNIPER and a Hopf bifurcation, we numerically study how it is modified in presence of coupling delay and noise, as well as in terms of changing the coupling strength.

The paper is organized as follows. In Section II, we present the details of the model and introduce the continuum limit formulation for the delay- and the noise-free setup, obtaining the Ott-Antonsen equation for the local order parameter. Proceeding along these lines, Section III contains the analytical results on the macroscopic stationary state and the related self-consistency equation derived for an arbitrary frequency distribution. In Section IV, the stability analysis is carried out by specifying a particular distribution of frequencies, comparing the results to numerical experiments. In Section V, it is further shown how the basic bifurcation scenario for the onset and the suppression of the collective mode is modified in presence of noise and coupling delay. Section VI contains a brief summary of the results obtained.

II. MODEL DYNAMICS AND THE CONTINUUM LIMIT FORMULATION

We consider a heterogeneous assembly of N globally coupled active rotators described by:

$$\begin{aligned} \dot{\theta}_i(t) = & \omega_i - a \sin \theta_i(t) - \frac{K}{N} \sum_j \sin(\theta_i(t) - \\ & \theta_j(t - \tau) + \alpha) + \sigma \eta_i(t), i = 1, \dots, N \end{aligned} \quad (1)$$

where the phase variables are $\theta_i \in S^1$, and the local dynamics is governed by the non-isochronicity parameter a and the natural frequency ω_i . Regarding the term "natural frequency", note that it will be used for convenience to describe the intrinsic parameter involving the quenched randomness, even though some units may exhibit excitable, rather than oscillatory behavior. The frequencies are distributed according to the probability density function $g(\omega)$ that satisfies $\int_{-\infty}^{\infty} g(\omega) d\omega = 1$, and is characterized by the mean value Ω and the variance Δ , which we here explicitly refer to as the *diversity* parameter. The individual unit rotates uniformly with the frequency ω_i for $a = 0$ only, whereas for $a > 0$ its rotation becomes non-uniform, having the rotation direction dependent on the sign of ω_i . The relation between ω_i and the parameter a underlies the excitability feature of autonomous dynamics. In particular, ω_i constitutes the bifurcation parameter, such that for fixed a , an isolated unit lies in the excitable regime if $|\omega_i| < a$. In this case, the unit possesses a stable node, whereas the characteristic nonlinear threshold-like response is mediated by an unstable steady state. At $|\omega_i| = a$, an isolated unit undergoes a SNIPER bifurcation toward the oscillatory regime. The interactions are assumed to be uniform across the population, and are characterized by the coupling strength K , the coupling phase-lag α and the coupling delay τ . The effect of random fluctuations is represented by the white Gaussian random forces η_i of intensity σ^2 , which act independently on each unit ($\langle \eta_i(t) \rangle = 0$, $\langle \eta_i(t) \eta_j(t) \rangle = \delta_{ij} \delta(t - t')$).

As already indicated, in this and the following section we apply the Ott-Antonsen framework [34, 35] to investigate the collective dynamics of an heterogeneous assembly of active rotators in the delay- and the noise-free case $\tau = \sigma = 0$. To this end, let us introduce the Kuramoto complex order parameter, which represents the center of mass of all rotators:

$$R(t) = r(t) e^{i\Psi(t)} = \frac{1}{N} \sum_j e^{i\theta_j(t)}, \quad (2)$$

such that (1) can be rewritten as

$$\dot{\theta}_i = \omega_i - \frac{a}{2i} (e^{i\theta_i} - e^{-i\theta_i}) + \frac{K}{2i} (R e^{-i(\theta_i + \alpha)} - \bar{R} e^{i(\theta_i + \alpha)}). \quad (3)$$

In the thermodynamic limit $N \rightarrow \infty$, the macroscopic state of the system can be described by the probability density function $f(\theta, \omega, t)$, which, for the considered

moment t , gives the relative number of oscillators whose phases and frequencies are $\theta_i(t) \approx \theta$, $\omega_k \approx \omega$. The normalization condition required for the probability density function is $\int_0^{2\pi} f(\theta, \omega, t) d\theta = 1$. Given the conservation of oscillators, $f(\theta, \omega, t)$ has to fulfill the continuity equation

$$\frac{\partial f}{\partial t} + \frac{\partial}{\partial \theta}(fv) = 0, \quad (4)$$

where the velocity is just

$$v(\theta, \omega, t) = \omega - \frac{a}{2i}(e^{i\theta} - e^{-i\theta}) + \frac{K}{2i}(Re^{-i(\theta+\alpha)} - \bar{R}e^{i(\theta+\alpha)}). \quad (5)$$

In the last expression, we have used the form of the Kuramoto mean field in the thermodynamic limit $N \rightarrow \infty$

$$R(t) = \int_{-\infty}^{\infty} g(\omega) d\omega \int_0^{2\pi} f(\theta, \omega, t) e^{i\theta} d\theta, \quad (6)$$

According to the Ott-Antonsen Ansatz [34, 35], the long-term dynamics of the continuity equation (8) tends to settle on a particular manifold of the form

$$f(\theta, \omega, t) = \frac{1}{2\pi} \left(1 + \sum_{n=1}^{\infty} \left[\bar{z}^n(\omega, t) e^{in\theta} + z^n(\omega, t) e^{-in\theta} \right] \right), \quad (7)$$

where the complex amplitude $z(\omega, t)$ is such that $|z(\omega, t)| \leq 1$. Introducing the assumption (7) into (4), one finds that $z(\omega, t)$ satisfies the Ott-Antonsen equation

$$\frac{dz}{dt}(\omega, t) = i\omega z + (1 - z^2) \frac{a}{2} + \frac{K}{2} Re^{-i\alpha} - \frac{K}{2} \bar{R} e^{i\alpha} z^2. \quad (8)$$

Note that $z(\omega, t)$ should be interpreted as the frequency-dependent *local order parameter*, in a sense that it quantifies the degree of synchrony of oscillators whose intrinsic frequencies $\theta_i \approx \omega$ lie within a small interval around the given frequency ω .

III. STATIONARY SOLUTION OF THE OTT-ANTONSEN EQUATION AND ITS STABILITY

In this section, our first goal is to determine the microscopic structure of the stationary state and the associated self-consistency equation. To do so, we look for the solutions of the Ott-Antonsen equation (8) for which the Kuramoto mean field $R(t) = r(t)e^{i\Psi(t)}$ is constant. In the next stage, we carry out the bifurcation analysis on the stability of the macroscopic stationary state, considering the scenarios that lead to the onset and the suppression of the collective mode. Proceeding with the first stage, let us substitute the assumption $z(\omega, t) = \rho(\omega, t)e^{i\phi(\omega, t)}$ into (8), which ultimately leads to

$$\begin{aligned} \dot{r} &= \frac{B}{2}(1 - r^2) \cos \phi, \\ r\dot{\phi} &= \omega r - \frac{B}{2}(1 + r^2) \sin \phi, \end{aligned} \quad (9)$$

having introduced the notation

$$\begin{aligned} B &= \sqrt{a^2 + K^2 \rho^2 + 2aK\rho \cos(\psi - \alpha)}, \\ \beta &= \arctan \frac{K\rho \sin(\psi - \alpha)}{a + K\rho \cos(\psi - \alpha)}, \\ \phi &= \varphi - \beta. \end{aligned} \quad (10)$$

From system (9), one infers that B , which depends only on the coupling strength and the mean field, plays the role of the *macroscopic excitability parameter*. This can be seen from the fact that the microscopic structure of the stationary state self-organizes in such a way that the assembly splits into two groups, according to the relation between the respective natural frequencies ω_i and B . In particular, group I is comprised of rotators in the *excitable regime*, whose intrinsic frequencies satisfy $|\omega| < B$, whereas group II consists of rotating units, whose intrinsic frequencies satisfy $|\omega| > B$. Another indication on the role of B can be obtained if the definitions of B and β from (10) are applied to transform the original equation for the dynamics of rotators (1) to $\dot{\theta}_i = \omega_i - B \sin(\theta_i - \beta)$, that just describes a set of forced active rotators. Perceived from the level of single units dynamics, B is then classically referred to as the *resistivity parameter*, in a sense that it measures the rotators ability to modify its natural frequency. Taking a more closer look at the dynamics of the two groups following from (9), one finds that for $|\omega| < B$, there exist two steady states, given by

$$\begin{aligned} r^*(\omega) &= 1, \\ \phi^*(\omega) &= \arcsin \frac{\omega}{B}, \end{aligned} \quad (11)$$

and

$$\begin{aligned} r^*(\omega) &= 1, \\ \phi^*(\omega) &= \pi - \arcsin \frac{\omega}{B}, \end{aligned} \quad (12)$$

whereby our stability analysis performed later on shows that only the solution (11) is stable. In case of the units within the rotating group $|\omega| > B$, the only steady state is

$$\begin{aligned} r^*(\omega) &= \frac{|\omega|}{B} - \sqrt{\frac{\omega^2}{B^2} - 1} \\ \phi^*(\omega) &= \frac{\pi}{2} \operatorname{sgn} \omega. \end{aligned} \quad (13)$$

Nevertheless, in order to fully quantify the stationary solution, one has to obtain an explicit expression for the macroscopic excitability parameter B . To do so, we invoke the self-consistency equation associated to the continuum form of the Kuramoto mean-field, which just derives from the definition (6) and the Ansatz (7):

$$R = \mathcal{G}z = \int_{-\infty}^{\infty} g(\omega) z(\omega) d\omega. \quad (14)$$

Applying (14) to the stationary state $z^*(\omega) = r^*(\omega)e^{i\phi^*(\omega)}$ given by (11) and (12), one obtains

$$\rho e^{i(\psi-\beta)} = \frac{i\bar{\omega}}{B} + \int_{|\omega|<B} d\omega g(\omega) \sqrt{1 - \frac{\omega^2}{B^2}} - \frac{i}{B} \int_{|\omega|>B} d\omega g(\omega) \omega \sqrt{1 - \frac{B^2}{\omega^2}}. \quad (15)$$

Separating for the real and the imaginary part of (15) and after some algebra, one ultimately arrives at the self-consistency equation for B of the form:

$$f(B) = B^2 - a^2 - 2K(f_1(B) \sin \alpha + f_2(B) \cos \alpha) + K^2 \frac{f_1^2(B) + f_2^2(B)}{B^2} = 0, \quad (16)$$

where

$$f_1(B) = \bar{\omega} - \int_{|\omega|>B} d\omega g(\omega) \omega \sqrt{1 - \frac{B^2}{\omega^2}},$$

$$f_2(B) = \int_{|\omega|<B} d\omega g(\omega) \sqrt{B^2 - \omega^2}. \quad (17)$$

Note that the analogous expression has been obtained in [28] for the particular case $a = 1, \alpha = 0$.

The results so far hold for an arbitrary distribution of natural frequencies $g(\omega)$. In order to perform the stability analysis on the stationary state and allow for the analytically obtained stability boundaries to be verified in numerical experiments, in the remainder we confine our study to the particular case of $g(\omega)$, conforming to a *uniform distribution of frequencies on a bounded interval*.

IV. STABILITY OF THE STATIONARY SOLUTION OF THE OTT-ANTONSEN EQUATION

As already announced, in this Section we specify the general results obtained so far by considering an example of a distribution of natural frequencies $g(\omega)$ which is uniform on a bounded interval $\omega \in [\omega_1, \omega_2]$:

$$g(\omega) = \begin{cases} 0, & \omega < \omega_1, \\ \gamma, & \omega_1 < \omega < \omega_2, \\ 0, & \omega > \omega_2, \end{cases} \quad (18)$$

where $\gamma = 1/(\omega_2 - \omega_1)$ comes from the standard normalization condition. This distribution is characterized by an average $\bar{\omega} = \frac{\omega_1 + \omega_2}{2}$ and the variance $\Delta = \omega_2 - \omega_1$. The advantage of such a choice of frequency distribution is that it allows for a full analytical treatment of the self-consistency equation (16). In particular, the integrals (17) are then explicitly given by

$$f_1(B) = \begin{cases} \bar{\omega} - \gamma(F_1(\omega_2) - F_1(\omega_1)), & B < \omega_1, \\ \bar{\omega} - \gamma F_1(\omega_2), & \omega_1 < B < \omega_2, \\ \bar{\omega}, & B > \omega_2, \end{cases} \quad (19)$$

where

$$F_1(\omega) = \frac{|\omega|}{2} \sqrt{\omega^2 - B^2} + \frac{B^2}{2} \ln \frac{B}{|\omega| + \sqrt{\omega^2 - B^2}}, \quad (20)$$

and

$$f_2(B) = \begin{cases} 0, & B < \omega_1, \\ \gamma(\frac{\pi}{4} B^2 - F_2(\omega_1)), & \omega_1 < B < \omega_2, \\ \gamma(F_2(\omega_2) - F_2(\omega_1)), & B > \omega_2, \end{cases} \quad (21)$$

with

$$F_2(\omega) = \frac{|\omega|}{2} \sqrt{B^2 - \omega^2} + \frac{B^2}{2} \arcsin \frac{\omega}{B}. \quad (22)$$

For the given $g(\omega)$ (18), we have carried out the stability and bifurcation analysis of the Ott-Antonsen equation (8), considering its linearization around the corresponding stationary solution (11)-(13). We take the cumulants of the frequency distribution, the mean $\bar{\omega}$ and the diversity Δ , as the main control parameters, while keeping the remaining parameters fixed. Note that for performing the stability analysis of (8), one has to rewrite it as a real system in order to eliminate the complex conjugation [38–40]. While the details of this calculation are explained in the Appendix, in the following we provide the main results on the stability boundaries of the stationary state, comparing them to what is obtained from numerical experiments on an assembly comprised of $N = 10^4$ active rotators.

It is convenient to interpret the analytical results in terms of how the number and the stability of the solutions of the self-consistency equation (16) for the macroscopic excitability parameter B change under variation of the control parameters. In particular, a typical form of the function $f(B)$ is illustrated in Fig. 1(a). Depending on the particular parameter values, it may possess either one of the three roots, denoted by $B_1 < B_2 < B_3$, which correspond to the stationary solutions of (16). Under variation of $\bar{\omega}$ and Δ , the system may undergo two saddle-node bifurcations, cf. the green lines in Fig. 1(b), where either B_1 and B_2 (upper green line) or B_2 and B_3 (lower green line) collide and disappear. The two branches of folds meet at the cusp point, where the pitchfork bifurcation occurs, see the inset in Fig. 1(b). Our stability analysis shows that the state B_3 is *always stable*, whereas the state B_2 is *always unstable*. At the other hand, the stability of the state B_1 is not affected only by the fold bifurcation, but may also change via Hopf bifurcation, indicated in Fig. 1(b) by the red dashed line.

The described bifurcation curves obtained by analyzing the stability of the stationary state of the Ott-Antonsen equation divide the $(\bar{\omega}, \Delta)$ parameter plane into several domains. In order to qualitatively understand the associated regimes of collective dynamics, we have carried out numerical simulations of the original system (1), having characterized the collective motion in terms of the time-averaged variance of the modulus of

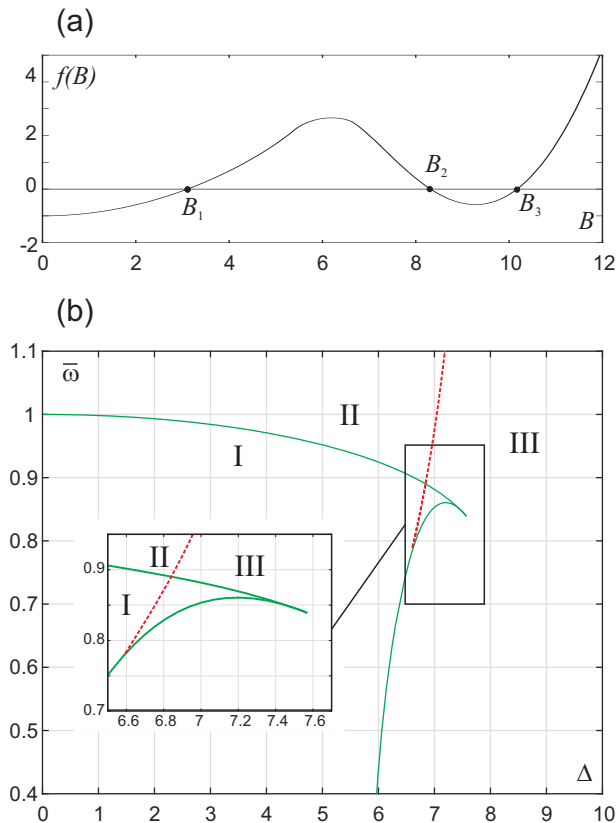


FIG. 1. (a) Typical solutions of the self-consistency equation (16) for B . The system parameters are: $a = 1$, $K = 5$, $\alpha = 0$, $\bar{\omega} = 0.8$ and $\Delta = 4$. (b) Bifurcation diagram constructed in the way described in the Appendix for $a = 1$, $K = 5$, $\alpha = 0$. The two branches of saddle-node bifurcations (green solid lines) emanate from the cusp point, where the pitchfork bifurcation occurs. The Hopf bifurcation curve is indicated by the red dashed line.

the Kuramoto mean-field $\rho(t) = |R(t)|$. In particular, the variance μ is defined as $\mu = \sqrt{\langle \rho^2 \rangle - \langle \rho \rangle^2}$, where the angled brackets denote the time-averaging, such that $\mu > 0$ indicates the oscillations of the mean field.

The dependence $\mu(\bar{\omega}, \Delta)$ with superimposed analytically obtained bifurcation curves is shown in Fig. 2(a), while the illustrative time-series of individual units and the mean-field $\rho(t)$ are provided in Fig. 2(b)-(e). One observes three characteristic regions, corresponding to (I) the global *rest state*, (II) the *synchronous state* and (III) the *asynchronous state*. In region I, none of the units is oscillating. Nevertheless, due to coupling, the rest state of each unit is shifted with respect to its position in the uncoupled case, whereby the shifts themselves are different as a consequence of diversity. Therefore, the mean field $\rho(t)$ is not exactly 1, but rather slightly less, cf. Fig. 2(c). At the boundary between the regions I and II, the collective dynamics undergoes a SNIPER bifurcation, which gives rise to long-period oscillations of the mean field. Then, all the oscillators are phase-locked and make synchronous revolutions around the circle, which

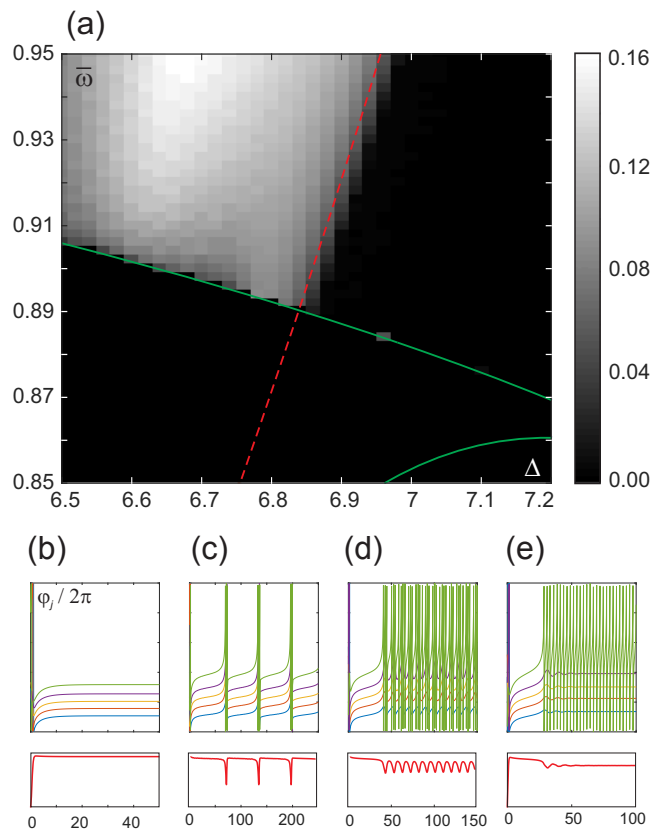


FIG. 2. (a) Variance μ in terms of Δ and $\bar{\omega}$, obtained by numerical simulations of an assembly consisting of $N = 10^4$ units for the parameters $a = 1$, $K = 5$, $\alpha = 0$. Superimposed are the analytically determined bifurcation curves from Fig. 1(b). (b)-(e) Illustration of the collective dynamics in the three characteristic parameter domains indicated in Fig. 1(b). The top row shows the time-series of phases of individual oscillators normalized over 2π , while in the bottom row are provided the corresponding time series $\rho(t) = |R(t)|$. Note that in the results are obtained for increasing diversity while $\bar{\omega} = 0.9$ is kept fixed. The particular values of diversity are $\Delta = 6$ in (b), $\Delta = 6.72$ in (c), $\Delta = 6.85$ in (d) and $\Delta = 7$ in (e).

induces sharp periodic beats of the mean field, see Fig. 2(d). As the diversity Δ increases further, more and more units lose entrainment, getting unlocked from the synchronized cluster, cf. Fig. 2(e). In the region III, the synchronization is completely lost, with some of the units exhibiting asynchronous oscillations while the other units lie at rest. The transition to the asynchronous state, i.e. the suppression of the collective mode, is analogous to the Kuramoto-type scenario of desynchronizing the system by increasing disorder, and is reflected by the Hopf bifurcation of the mean field. Note that the sequence of transitions from region I to III via synchronous state II with increasing diversity alone can be observed only if the mean frequency $\bar{\omega}$ is large enough. Otherwise, the transition from the rest state to asynchronous state under increasing heterogeneity does not involve the synchronous state. In general, we have established that the

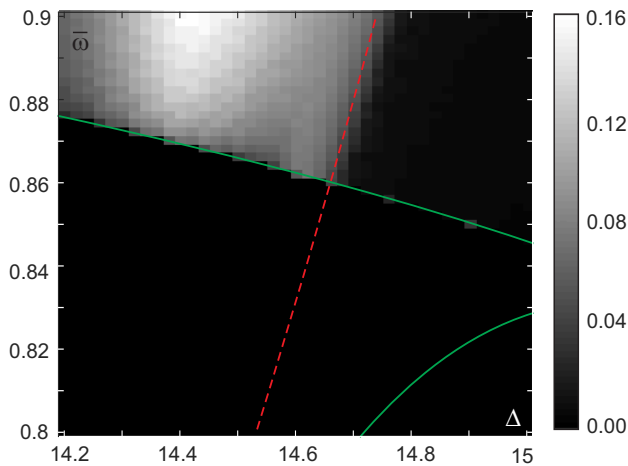


FIG. 3. (a) Variance μ in terms of Δ and $\bar{\omega}$ for the parameters $a = 1$, $K = 7$, $\alpha = 0$. The corresponding analytically determined bifurcation curves obtained within Ott-Antonsen framework are presented in the same style as in Fig. 2(a).

comparison between the analytical predictions for the bifurcation curves outlining the domain boundaries and the corresponding results of numerical simulations shows excellent agreement.

We have also examined whether the qualitative picture described above is affected by varying the coupling strength K . It has been verified that the general structure of the phase space remains qualitatively the same, i.e. the bifurcation scenario underlying transitions between the three different regimes of collective motion is generic. Still, one observes that for increasing coupling strength, the cusp point and the Hopf bifurcation curve outlining the suppression of the collective mode shift to larger diversity, cf. Fig. 3 and Fig. 2(a).

V. THE IMPACT OF COUPLING DELAY AND NOISE

In this section, we employ extensive numerical simulations to investigate whether and how is the bifurcation scenario for the onset and the suppression of the collective mode discussed so far modified in the presence of coupling delay or noise. In both instances, we shall compare the numerically obtained fields $\mu(\bar{\omega}, \Delta)$ with the bifurcation curves obtained analytically for the *delay- and noise-free case*.

The typical effects of explicitly incorporating the coupling delay are illustrated in Fig. 4(a), which shows the dependence $\mu(\bar{\omega}, \Delta)$ for $\tau = 0.5$. The presence of coupling delay naturally does not affect the coordinates of the steady states. Therefore, the saddle-node bifurcation curves are not altered by the coupling delay. Nevertheless, the key effect of the delay is that the Hopf bifurcation underlying the suppression of the collective mode shifts to smaller diversity. This implies that the

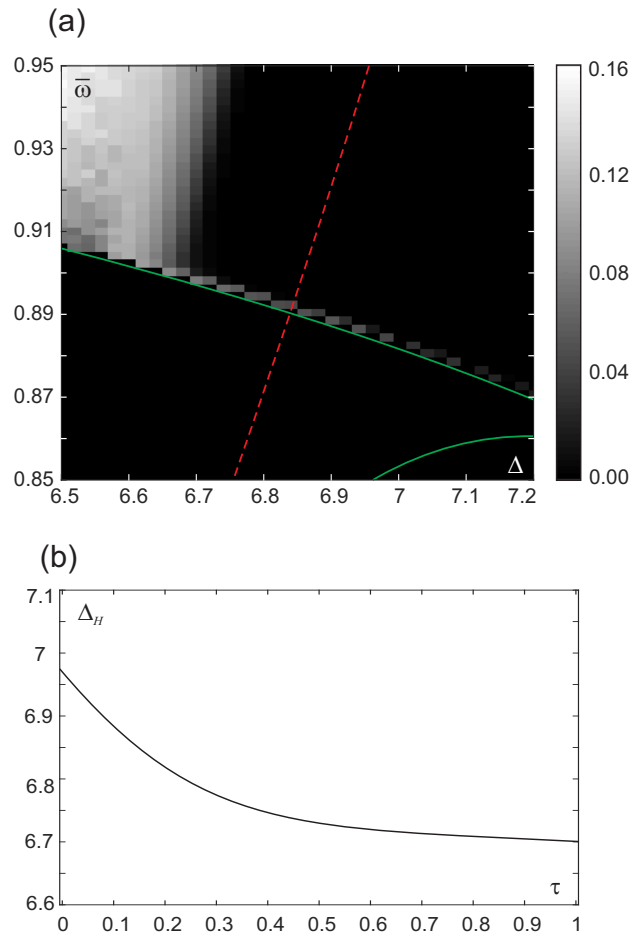


FIG. 4. (a) Dependence $\mu(\bar{\omega}, \Delta)$ obtained for coupling delay $\tau = 0.5$ and the remaining parameters fixed to $a = 1$, $K = 5$, $\alpha = 0$, the same as in Fig. 1(b). Superimposed are the analytically determined bifurcation curves for the delay- and noise-free case from Fig. 1(b). (b) Critical diversity Δ_H corresponding to the Hopf bifurcation in dependence of τ for fixed $\bar{\omega} = 0.88$.

coupling delay may effectively *quench the macroscopic oscillations*, stabilizing the fixed point of the collective dynamics. In Fig. 4(b) is demonstrated how the critical diversity Δ_H where the Hopf bifurcation takes place declines with the coupling delay τ when all the remaining parameters are kept fixed.

In contrast to the impact of coupling delay, the presence of noise is established to primarily influence the *saddle-node bifurcations* obtained for the $\tau = \sigma = 0$ case. In qualitative terms, noise acts in two antagonistic ways: applying a small amount of local noise may stimulate some of the excitable units to become oscillatory, thus promoting a synchronized firing, while on the other hand, having a too strong local noise has a detuning effect. Figure 5(a) illustrates the dependence $\mu(\bar{\omega}, \Delta)$ obtained for the moderate noise intensity $\sigma^2 = 0.09$. In this case, one finds that the location of both the SNIPER and the Hopf bifurcation are shifted compared to the deterministic case, depending on the noise intensity. In particular,

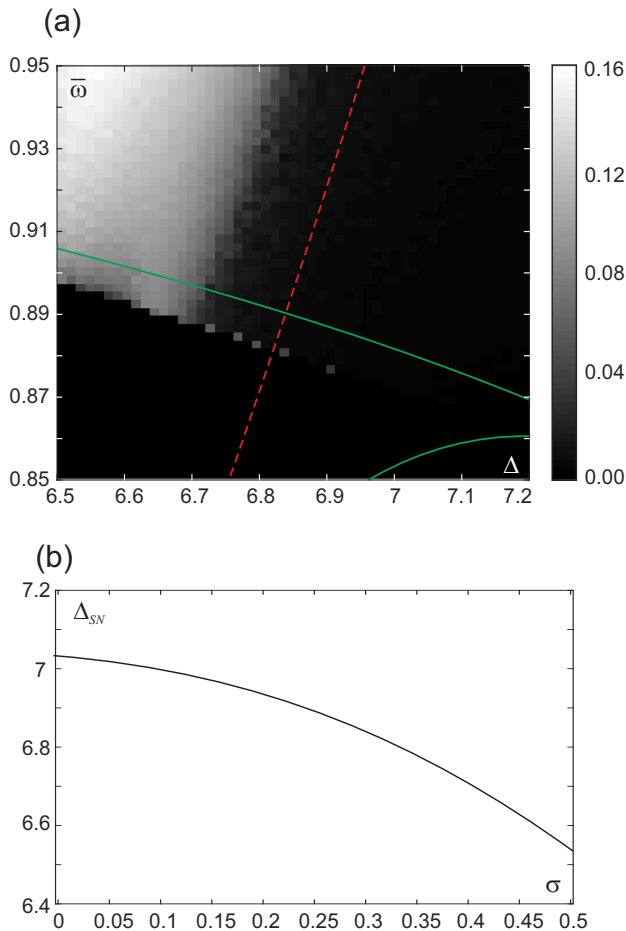


FIG. 5. (a) Field $\mu(\bar{\omega}, \Delta)$ obtained for $\sigma = 0.3$, while keeping the remaining parameters fixed at $a = 1$, $K = 5$, $\alpha = 0$, the same values as in Fig. 1(b). Superimposed are the analytically determined bifurcation curves for the deterministic system. (b) Decrease of the critical diversity Δ_{SN} corresponding to the SNIPER bifurcation with σ for fixed $\bar{\omega} = 0.88$.

the primary effect of the *small* noise is to promote synchronized firing, i.e. the onset of the collective mode, which is effectively analogous to increasing $\bar{\omega}$. As a consequence, one observes that the critical diversity Δ_{SN} at which the SNIPER bifurcation takes place reduces under increasing noise intensity, as indeed shown in Fig. 5(b) for the fixed $\bar{\omega} = 0.88$. However, introducing the *intermediate* noise has an additional pronounced impact on the Hopf bifurcation. In this case, the disorder in the system is increased, which effectively precipitates the transition from the synchronous to asynchronous regime, enforcing it to occur at the smaller diversity.

VI. SUMMARY AND CONCLUSION

In the present paper, we have analyzed the scenarios for the onset and the suppression of the collective mode in a heterogeneous assembly, where the active rotators in the excitable or the oscillatory regime are subjected to

noise and/or coupling delay. The main ingredients of the model, including diversity, coupling delay and noise are typical for neuronal and other biological systems. Our study has first been focused on analytically treating the delay- and noise-free case in the continuum limit, having then numerically examined how the obtained bifurcation scenario is modified in presence of noise and coupling delay. The analytical part of the study has been carried out within the framework of Ott-Antonsen theory, which allowed us to determine the macroscopic stationary state, i.e. the state with the constant mean field, in case of an arbitrary distribution of natural frequencies. The main insight into the microscopic structure of such a state is that the population splits into the excitable and the rotating group, depending on the relation between the units natural frequency and the macroscopic excitability parameter. The stability analysis on the stationary state has been performed by considering the particular case of a uniform frequency distribution on a bounded interval, which enabled us to analytically construct the corresponding bifurcation diagrams, with the cumulants of the frequency distribution being the main control parameters. While the stationary state has been determined earlier for a similar, but less general model [28], the stability analysis, as presented here, has been carried out for the first time.

We have demonstrated that the collective dynamics may exhibit three qualitatively different regimes, including the rest state, the synchronous state and the asynchronous state. The underlying bifurcation structure is essentially organized by a SNIPER and a Hopf bifurcation curve, whereby the former corresponds to a transition from the macroscopic rest state to the synchronous regime, while the latter accounts for the Kuramoto-type scenario of transition from synchronous to asynchronous state due to increasing disorder, reflected in the diversity of natural frequencies. By carrying out extensive numerical simulations, we have shown that this basic bifurcation structure persists in presence of noise and coupling delay. Nevertheless, the noise and the coupling delay are found to effectively shift the position of the bifurcation curves with respect to the noise- and delay-free case, such that the noise affects both the SNIPER and the Hopf bifurcation, whereas the delay primarily influences the Hopf bifurcation. In particular, applying a small noise is found to primarily promote synchronized firing, reducing the diversity threshold necessary for the onset of the collective mode. Nevertheless, introducing intermediate noise imposes a disordering effect, which manifests itself in that the transition from synchronous to asynchronous regime occurs at smaller diversity. At the other hand, the coupling delay is seen to have a stabilizing effect with respect to the rest state, effectively quenching the onset of the collective mode by reducing the diversity threshold for the desynchronization transition. While the described bifurcation structure appears to be generic for the considered type of frequency distribution, remaining qualitatively similar under the influence of noise and coupling

delay, it will be interesting to examine whether and how it is modified if one considers other forms of frequency distribution, such as a bimodal one.

Appendix: Calculation of the stability of the stationary solution of the Ott-Antonsen equation

Here we elaborate on how one can calculate the stability of the stationary solution of the Ott-Antonsen equation (8). In particular, we first introduce the expressions $z(\omega, t) = x(\omega, t) + iy(\omega, t)$ and $R(\omega, t) = X(\omega, t) + iY(\omega, t)$ for the local and the global order parameter, respectively, transforming (8) to

$$\begin{aligned} \dot{x} &= F(x, y, X, Y) = \frac{a}{2}(y^2 - x^2 + 1) - \omega y - \\ &\quad - Kxy(Y \cos \alpha - X \sin \alpha) - \frac{K}{2}(X \cos \alpha + Y \sin \alpha) \cdot \\ &\quad \cdot (x^2 - y^2) + \frac{K}{2}(X \cos \alpha + Y \sin \alpha) \\ \dot{y} &= G(x, y, X, Y) = -axy + \omega x - Kxy(Y \sin \alpha + X \cos \alpha) + \\ &\quad + \frac{K}{2}(Y \cos \alpha - X \sin \alpha)(x^2 - y^2) + \\ &\quad + \frac{K}{2}(Y \cos \alpha - X \sin \alpha). \end{aligned} \quad (\text{A.1})$$

The linearization of the Ott-Antonsen equation (8) for variations $\xi(t) = (x_1(t), y_1(t))^T$, $\Xi(t) = (X_1(t), Y_1(t))^T$ of the stationary solution (x_0, y_0) can then succinctly be written in the matrix form as

$$\frac{d\xi(\omega, t)}{dt} = A(\omega)\xi(\omega, t) + B(\omega)\Xi(t), \quad (\text{A.2})$$

where the matrices of derivatives are

$$A(\omega) = \begin{pmatrix} \frac{\partial F}{\partial x} & \frac{\partial F}{\partial y} \\ \frac{\partial G}{\partial x} & \frac{\partial G}{\partial y} \end{pmatrix}, \quad B(\omega) = \begin{pmatrix} \frac{\partial F}{\partial X} & \frac{\partial F}{\partial Y} \\ \frac{\partial G}{\partial X} & \frac{\partial G}{\partial Y} \end{pmatrix}. \quad (\text{A.3})$$

Assuming that the variation $\xi(\omega, t)$ satisfies the Ansatz $\xi(\omega, t) = \xi_1(\omega)e^{\lambda t}$, (A.2) becomes

$$(A(\omega) - \lambda I)\xi(\omega, t) + B(\omega)\Xi(t) = 0, \quad (\text{A.4})$$

where I denotes the identity matrix. Multiplying (A.4) from the left by $g(\omega)(A(\omega) - \lambda I)^{-1}$ and integrating over ω , one finds that $C(\lambda)\Xi = 0$, where

$$C(\lambda) = I + \int_{-\infty}^{\infty} d\omega g(\omega)(A(\omega) - \lambda I)^{-1} B(\omega). \quad (\text{A.5})$$

Therefore, the Lyapunov spectrum characterizing the stability of the stationary solution can be obtained by numerically solving the system $\det C(\lambda) = 0$.

ACKNOWLEDGMENTS

This work was supported by the Russian Foundation for Basic Research under project Nos. 17-02-00904 and 19-52-10004, as well as the Ministry of Education, Science and Technological Development of Republic of Serbia under project No. 171017. The authors would like to thank Matthias Wolfrum for fruitful discussions during the various stages of the study.

-
- [1] A. Pikovsky, M. Rosenblum, and J. Kurths, *Synchronization: A Universal Concept in Nonlinear Sciences* (Cambridge University Press, Cambridge, 2003).
- [2] J. A. Acebrón, L. L. Bonilla, C. J. P. Vicente, F. Ritort, and R. Spigler, *Rev. Mod. Phys.* **77**, 137 (2005).
- [3] Y. Baibolatov, M. Rosenblum, Z. Z. Zhanabaev, M. Kyzgarina, and A. Pikovsky, *Phys. Rev. E* **80**, 046211 (2009).
- [4] I. Franović, K. Todorović, N. Vasović and N. Burić, *Phys. Rev. E* **87**, 012922 (2013).
- [5] S. Olmi, R. Livi, A. Politi, and A. Torcini, *Phys. Rev. E* **81**, 046119 (2010).
- [6] L. S. Tsimring, and A. Pikovsky, *Phys. Rev. Lett.* **87**, 250602(2001).
- [7] A. Pototsky, and N. B. Janson, *Phys. Rev. E* **77**, 031113 (2008).
- [8] A. Zakharova, S. A. M. Loos, J. Siebert, A. Gjurchinovski, J. C. Claussen, E. Schöll, Controlling Chimera Patterns in Networks: Interplay of Structure, Noise, and Delay in E. Schöll, S. H. L. Klapp, P. Hövel, (eds), *Control of Self-Organizing Nonlinear Systems* (Springer International Publishing, Switzerland, 2016).
- [9] S. Strogatz, *Physica D* **143**, 1 (2000).
- [10] N. Komin, and R. Toral, *Phys. Rev. E* **82**, 051127 (2010).
- [11] C. J. Tessone, A. Scirè, R. Toral, and P. Colet, *Phys. Rev. E* **75**, 016203 (2007).
- [12] D. Pazo, and E. Montbrió, *Phys. Rev. E* **73**, 1 (2006).
- [13] F. M. Atay, ed., *Complex Time-Delay Systems: Theory and Applications* (Springer, Berlin, Heidelberg, (2010)).
- [14] E. Schöll, G. Hiller, P. Hovel, and M. A. Dahlem, *Phil. Trans. R. Soc. A* **367**, 1079 (2009).
- [15] A. Takamatsu, T. Fujii, I. Endo, *Phys. Rev. Lett.* **85**, 2026 (2000).
- [16] M. G. Rosenblum and A. S. Pikovsky, *Phys. Rev. Lett.* **92**, 114102 (2004).
- [17] P. Perlikowski, S. Yanchuk, O. Popovych, and P. Tass, *Phys. Rev. E* **82**, 036208 (2010).
- [18] B. Lindner, J. Garca-Ojalvo, A. Neiman, and L. Schimansky-Geier, *Phys. Rep.* **392**, 321 (2004).
- [19] V. Klinshov, and I. Franović, *Phys. Rev. E* **92**, 062813 (2015).
- [20] I. Franović, and V. Klinshov, *Chaos* **28**, 023111 (2018).
- [21] I. Franović, and V. Klinshov, *EPL* **116**, 48002 (2016).
- [22] I. Franovic, and V. Klinshov, *Eur. Phys. J. - Spec. Top.* **227**, 1063 (2018).
- [23] I. Franović, K. Todorović, M. Perc, N. Vasović, and N. Burić, *Phys. Rev. E* **92**, 062911 (2015).

- [24] I. Franović, M. Perc, K. Todorović, S. Kostić, and N. Burić Phys. Rev. E **92**, 062912 (2015).
- [25] I. Bačić, V. Klinshov, V. I. Nekorkin, M. Perc, and I. Franović, EPL **124**, 40004 (2018).
- [26] F. A. Rodrigues, T. K. DM. Peron, P. Ji, and J. Kurths, Phys. Rep. **610**, 1 (2016).
- [27] C. J. Tessone, C. R. Mirasso, R. Toral, and J. D. Gunton, Phys. Rev. Lett. **97**, 194101 (2006).
- [28] L. F. Lafuerza, P. Colet, and R. Toral, Phys. Rev. Lett. **105**, 084101 (2010).
- [29] S. Kadar, J. Wang, and K. Showalter, Nature London **391**, 770 (1998).
- [30] S. Alonso et al., Phys. Rev. Lett. **87**, 078302 (2001).
- [31] D. E. Potsnov, S. K. Han, T. G. Yim, and O. V. Sosnovtseva, Phys. Rev. E **59**, R3791 (1999).
- [32] M. A. Zaks, A. B. Neiman, S. Feistel, and L. Schimansky-Geier, Phys. Rev. E **68**, 066206 (2003).
- [33] M.Y. Choi, H.J. Kim, D. Kim, H. Hong, Phys. Rev. E **61**, 371 (2000).
- [34] E. Ott and T. M. Antonsen, Chaos **18**, 037113 (2008).
- [35] E. Ott and T. M. Antonsen, Chaos **19**, 023117 (2009).
- [36] I. V. Tyulkina, D. S. Goldobin, L. S. Klimenko, and A. Pikovsky, Phys. Rev. Lett. **120**, 264101 (2018).
- [37] D. S. Goldobin, I. V. Tyulkina, L. S. Klimenko, and A. Pikovsky, Chaos **28**, 101101 (2018).
- [38] M. Wolfrum, S. V. Gurevich, and O. E. Omel'chenko, Nonlinearity **29**, 257 (2016).
- [39] O. E. Omelchenko, and M. Wolfrum, Physica D **263**, 74 (2013).
- [40] O. E. Omel'chenko, and M. Wolfrum, Phys. Rev. Lett. **109**, 164101 (2012).